Journal of Thermal Analysis, Vol. 48 (1997) 373-383

EFFECT OF MECHANICALLY MIXED ZnO ON THE EVOLUTION OF PORE STRUCTURE OF SiO_2 UPON THERMAL TREATMENT

Gamal M. S. El Shafei[1]*, *Christine A. Philip*[1] *and Zinab A. Omran*[2]

[1]Ain Shams University, Faculty of Science, Chemical of Department, Abbassia, Cairo
[2]Benha University, Faculty of Science, Chemical of Department, Benha, Egypt

Abstract

N_2 adsorption at 77 K was used to follow the change in the pore structure of silica (mesoporous) produced on heating at 300 and 600°C in the presence of different contents of mechanically mixed ZnO (15–85 mol%).

Heating of pure silica at 300°C caused pore narrowing. This proceeded differently in the presence of ZnO, the pore system being split into two ranges of limited sizes. The pore widening effect upon heating silica at 600°C was greatly reduced upon the addition of ZnO, to the extent of the evolution of some micropores at low levels of ZnO.

At both heating temperatures, the composition 30% ZnO represented a transient state through the flux of pore system change. The IR spectra indicated that at this composition the silica particles are more oblate.

The pore structure variations due to heating at the examined temperatures correlated with the solid-state reactions that take place at 1000°C, where the spinel Zn_2SiO_4 is detected.

Keywords: mechanical mixture, pore structure, SiO_2–ZnO

Introduction

Processes involving the chemical transformation of solids are playing an increasingly important role in modern technology, as in this way sophisticated and costly solids can be produced by the reactions of precursory solids.

Oxidic spinels have been found to have interesting electrical and catalytic properties and also important technological applications [1–3], especially in electronic devices and as refractories in the heavy industries [4].

As the solid-state reactions are bulk diffusion-controlled, a firm correlation with pore structure should emerge. Gas adsorption remains the most successful method of giving a near-real description of the porous structure [5].

In this study, N_2 adsorption at 77 K was used to characterize the changes induced in the pore structure of silica upon the addition of ZnO and thermal treat-

---

* Author to whom all correspondence should be addressed.

0368–4466/97/ $ 5.00

John Wiley & Sons Limited
Chichester

ment. ZnO–SiO_2 mixtures with a wide range of composition (15–85 mol%) were prepared by mechanical mixing, and subjected to heating at 300 or 600°C in air.

Experimental

The parent oxides were 99.5 purity (BDH). Appropriate amounts of oxides were finely divided in a porcelain mortar, and bidistilled water was then added to the mixture in a slow stream with vigorous stirring to ensure complete homogeneity. The wet mixtures were dried for 5 h at 115°C in air, and only the specimens collected between 100 and 200 mesh sizes were used. The powders thus obtained were heated for 5 h at 300 or 600°C in air, cooled in a desiccator and kept in covered glass tubes under vacuum. Five compositions were prepared: 15, 30, 50, 70 and 85 mol% SiO_2, which will be designated I, II, III, IV and V, respectively. The heating temperature will be indicated between parentheses.

A conventional volumetric apparatus was used to obtain the adsorption-desorption isotherms of N_2 at 77 K, connected to a vacuum system that permits a prior outgassing to a residual pressure of 10^{-4} Torr.

IR spectra were obtained on a Pye-Unicam SP3-200A spectrometer in the range 4000–600 cm^{-1}, the KBr disc technique being used.

Results and discussion

Sorption characteristics are described following the BDDT isotherm classification [6], and IUPAC recommendations [7] for the type of hysteresis. The specific surface area was estimated by application of the BET equation, A_{BET}, in its normal range of applicability, with a value of 16.2 $Å^2$ for the cross-sectional area of N_2. The total pore volume, V_p, was taken at $p/p^o=0.95$ as liquid volume, and the average pore radius, r_H, was calculated as V_p/A_{BET} (pp) or $2V_p/A_{BET}$.(c_p).

Porosity determination was accomplished by constructing the V *vs.* t plots, in which we selected the reference t values of Lecloux *et al.* [8], depending on the value of the BET C constant. The correct choice of the reference data was judged through the agreement between the area calculated from the plot, A_t, and A_{BET}. Pore size distribution was inspected by using the corrected modelless method [9]. Criteria such that agreement between the calculated (cumulative) and experimental parameters of area and volume [9] and the IUPAC recommendation [7] governed the choice of the pore model; either c_p or *pp*, and the isotherm branch; either adsorption or desorption. In all cases, the calculations were extended until the correction term proposed by the method was equal to or exceeded the volume desorbed. While the agreement between V_{cum} and V_p was excellent in all cases, within a few percent, the area parameters exhibited differences greater than the acceptable range; reasons are attributed to these differences in each case.

Parent oxides

The adsorption isotherm of the parent silica was of type IV, i.e. for a mesoporous solid, in which the desorption branch formed a type H1 hysteresis loop with two sloping branches that narrowed before closing at $p/p^0=0.32$ (Fig. 1a). The mesopores present can therefore be described as tubular pores open at both ends, with openings of effective and varying radii; the narrowness at the lower part infers the presence of some ink-bottle character [10].

Heating at 300°C caused a change in the isotherm shape, whereby it became of type II with an H3 hysteresis loop that closed at $p/p^0=0.22$. This hysteresis type is attributed to an assembly of slit-shaped capillaries [7]; moreover, the extension of the hysteresis loop to a low value (<0.4) of p/p^0 is taken as an indication of the presence of barely accessible entrances [11]. This is reflected in the value of the average pore radius, r_H, where it is decreased to nearly half the initial value, a situation arising because no change in A_{BET} has taken place, whereas V_p has been reduced markedly (Table 1).

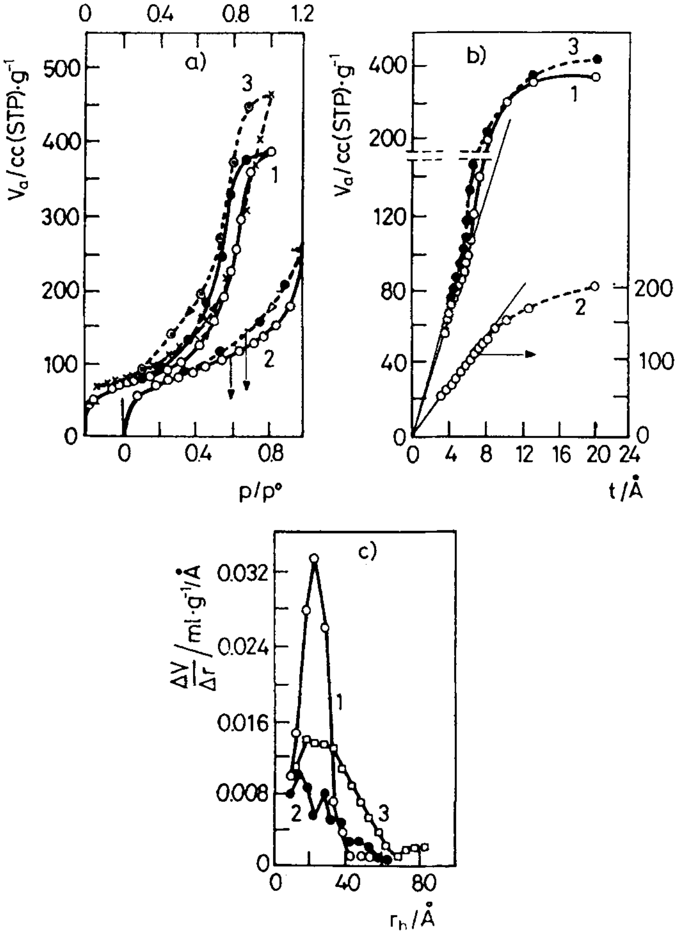

Fig. 1 N$_2$ adsorption-desorption isotherms [a]; V–t plots [b] and pore size distribution curves [c] for parent unheated silica ①; silica (300) ②: and silica (600) ③

When the temperature was raised to 600°C, the silica showed a type IV isotherm with two differences relative to the parent: the hysteresis loop was wider throughout the covered p/p^o range, and the adsorption branch displayed a higher slope on reaching $p/p^o=1.0$ (Fig. 1a). These differences infer that pore widening has taken place, which agrees with the increase in the value of r_H (Table 2).

The *V vs. t* plot for the unheated sample (Fig. 1b) shows that the first group of points up to $t=5.9$ Å($p/p^o=0.50$) lie on the straight line that extends through the origin; an upward deviation then commences at $t=6.0$ Å ($p/p^o=0.53$) and continues up to $t=12.7$ Å ($p/p^o=0.9$), where the volume adsorbed reaches nearly a constant value. This upward deviation therefore represents the mesoporous character of the solid, but the delay in this deviation [the hysteresis loop closes at $p/p^o=0.32$] may be interpreted as a compensation effect [12]. The presence of some narrow pores (super micropores) filled by multilayer formation resulted in a downward deviation that opposed the corresponding upward deviation expected from the mesopores (of limited sizes) in this region of the plot. Upon heating at 300°C, this upward deviation was greatly reduced, whereby the points up to $t=8.0$ Å ($p/p^o=0.75$) lay on the straight line that passes through the origin, followed by a downward deviation (Fig. 1b). Heating at 300°C caused a narrowing of the pores, resulting in the evolution of some micropores besides making the existing mesopores of limited sizes. In contrast, heating at 600°C seemed to cause pore widening, the *V vs. t* plot showing an upward deviation that started at $t=5.0$ Å ($p/p^o=0.34$), which matched the closure point of the hysteresis loop (Table 2). This means that the narrow pores which caused the compensation effect in the case of the unheated sample disappeared upon heating at 600°C via pore widening, as can be seen in the plot for $t>12$ Å (Fig. 1b).

The pore size distribution curve for the unheated sample, calculated from the adsorption branch, exhibited a maximum at a hydraulic pore radius, r_h, of 22.5 Å on the basis of parallel plate idealization, i.e. the most frequent pores are those with a width of 45 Å (Fig. 1c). The value of V_{cum} shows good agreement with V_p, but A_{cum} is 23% higher then A_{BET} (Table 1); such a difference is far from being acceptable as a criterion of agreement. De Boer [13] mentioned a number of reasons why A_{cum} may be greater than A_{BET}. The pores may intersect and the volume of intersections is not bounded by the surface of the solid, but it is included in the calculation of A_{cum}; in the case of pores with widened and narrow parts, the volume of these parts is attributed to pores that are narrower.

The curve of the sample heated at 300°C, based on the parallel plate, indicated that a drastic decrease in the number of pores with $r_h=12.5$–30.0 Å took place upon heating. The curve shows two maxima, at $r_h=12.5$ Å and 27.5 Å, with a predominance of the former. Such a predominance is in line with the proposed pore narrowing arrived at above. On the other hand, the appearance of another maximum at a larger size may be a consequence of the pore narrowing process, where some of the mesopores and their mouths become wider through the movement of the bulk material to enclose a narrower size (Fig. 1c). This is presumably the reason for the constancy of A_{BET} (Table 1). The loss in area expected from the pore

Table 1 Surface characteristics of SiO_2–ZnO (300) characteristics

Sample	A_{BET}/ $m^2\ g^{-1}$	A_t/ $m^2\ g^{-1}$	BET C-const.	V_p/ ml g^{-1}	r_H^{pp}/ Å	A_{cum}^{pp}/ $m^2\ g^{-1}$	V_{cum}^{pp}/ ml g^{-1}	A_n/ $m^2\ g^{-1}$	$\frac{A_n}{A_{BET}}$	Hyst. clos. point (p/p^0)
SiO_2	258	258	106	0.5812	22.5	318	0.6068	–	–	0.32
SiO_2 (300)	261	261	100	0.3177	12.2	151	0.3099	110	0.42	0.22
I	37.7	37	48	0.0790	21.0	37	0.0826	–	–	0.53
II	113	115	58	0.1294	11.4	53	0.1255	60	0.53	0.50
III	182.5	185	49	0.2325	12.7	107.5	0.2326	75	0.41	0.40
IV	183	189	119	0.2433	13.3	137.5	0.2341	45.5	0.25	0.50
V	204.5	208	106	0.2604	12.7	128.5	0.2643	76	0.37	0.28

Table 2 Surface characteristics of SiO_2–ZnO (600) series

Sample	A_{BET}/ $m^2\ g^{-1}$	A_t/ $m^2\ g^{-1}$	BET C-const.	V_p/ ml g^{-1}	r_H^{pp}/ Å	A_{cum}^{pp}/ $m^1\ g^{-1}$	V_{cum}^{pp}/ ml g^{-1}	A_n/ $m^2\ g^{-1}$	$\frac{A_n}{A_{BET}}$	Hyst. clos. point (p/p^0)
SiO_2 (600)	271	267	267	0.6510	48	306	0.6288	–	–	0.32
I	33.5	32	42	0.0790	23.6*	40*	0.0815*	–	–	0.48
II	65.5	67	83	0.1007	30.8	59.5	0.0998	6	0.09	0.48
III	95.5	91	98	0.1395	29.2	77.5	0.1368	18	0.19	0.35
IV	170	172	128	0.2232	26.2	112	0.2134	58	0.34	0.45
V	181.5	188	80	0.1868	20.6	128	0.1887	53.5	0.29	0.22

* Parallel plate idealization.

narrowing is compensated by the exposure of more area through pore widening. Nevertheless, because the number of wide pores is low (relative to the unheated sample), a significant decrease occurred in V_p (Table 1). Although V_{cum} was about 97.5% of V_p, A_{cum} was only about 58% of A_{BET}. It must be emphasized that the calculations were continued down to $p/p^o=0.25$, using the desorption data; the adsorption data resulted in larger discrepancies in both volume and area. This lower A_{cum} is therefore evidence of the evolution of some barely accessible micropores [14]. With adoption of a cylindrical pore shape for the adsorption branch data, the distribution curve for the sample heated at 600 °C showed that heating at 600°C caused a decrease in the number of pores with sizes in the range $r_h=12.5$–27.5 Å (Fig. 1c). Moreover, the pores with $32.5 \leq r_h \leq 62.5$ Å increased in number, these groups of pores may be responsible for the increase in V_p relative to the unheated sample (Table 2). V_{cum} for this sample was 3% lower than V_p, but A_{cum} was 12% higher than A_{BET}. As the difference between A_{cum} and A_{BET} has previously been attributed to the narrower parts in the pore system, the decrease in this difference can be taken as an indication of the decrease in the narrower parts that were originally present. These narrower parts could disappear via rounding of the pores at their edges, so that readier access to the wider capillaries is achieved, which may account for the marked increase in the value of the BET *C*-constant (Table 2).

The ZnO sample yielded an isotherm of type II, characterized by a very small uptake in the p/p^0 range 0.1–0.8, followed by a steep increase only near $p/p^o=1$. The calculated area was <5 m^2/g, which is a highly suspicious value in view of the precision proposed in the used technique. In other words, this oxide probably exposes very wide pores that required another probe than N_2 to give a more confident value of area. On the other hand, the presence of very fine pores can not be ruled out, but they are certainly inaccessible to N_2. Heating at either 300 or 600°C decreased the adsorptive capacity of the solid drastically.

SiO_2–ZnO(300)

All the isotherms of this group were of type II, exhibiting a hysteresis loop that closed in the range ~0.3–0.5 for p/p^o, showing no specific trend (Table 1). A progressive decrease in A_{BET} accompanied the increase in ZnO content, and a corresponding one took place in V_p; consequently, r_H remained practically constant up to 70% ZnO. At 85% ZnO, drastic decreases in both area and volume occurred, but the average pore radius had a value that approached r_H for the parent (unheated) silica.

The *V vs. t* plot for sample V (15% ZnO) (Fig. 2) showed no deviations up to $t=7$ Å ($p/p^o=0.65$), after which a downward deviation took place. For samples IV–II, the plots were similar in the sense that they exhibited a downward deviation, followed by an upward turning, without going above the straight line passing through the origin. However, the downward deviation displayed an increasing departure, following the sequence IV<III<II. The plot for sample I indicated the presence of mesopores only.

The hysteresis loop in the isotherm of sample *V* closed at p/p^o~0.3 (Table 1). Thus, the long straight portion in its *V vs. t* plot (up to $p/p^o=0.65$) indicated a situation of a compensation effect; if this is compared with the parent (unheated) silica, it can be seen to result from an increase in the extent of narrow pores at the expense of the mesopores. The downward deviations in the *V vs. t* plots, as discussed by Lippens and De Boer [15], signify that a part of the surface has become unavailable because some narrow pores are filled up by multilayer adsorption. Accordingly, from the increase in this downward deviation from sample IV to sample II, it can be seen that the unavailable surface due to the increase in pore narrowing increases in that sequence; on the other hand, the behaviour of the upward turning reflects the size of the mesopores present (Table 1). For sample I, the micropores, if present, are inaccessible to N_2, but the mesopores present are larger than for the other four samples, as reflected by the value of r_H (Table 1).

The cumulative parameters extracted from pore structure analysis of the desorption branch (parallel plate shape) are given in Table 1. For all samples, there was a satisfactory agreement between V_{cum} and V_p, while A_{cum} for all samples except sample I (which displayed excellent agreement) was lower than the corresponding A_{BET}. The lower value of A_{cum}, as mentioned before, is attributed to the presence of barely accessible narrow pores.

The evolution of the narrow pore fraction A_n/A_{BET} exhibited a continuous decrease upon increase of the ZnO content up to 30% [Sample IV]; it then increased

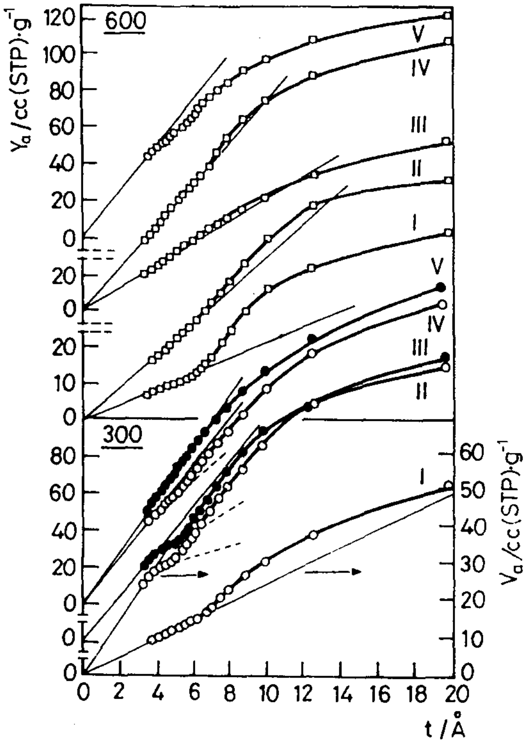

Fig. 2 *V–t* plots of different SiO_2–ZnO samples

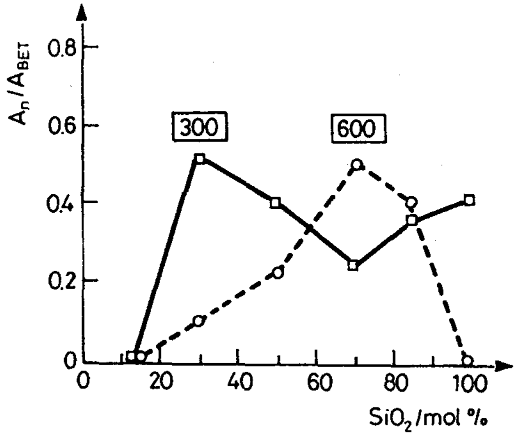

Fig. 3 Change of narrow pores fraction as a function of SiO_2 content

with the further increase of ZnO (Fig. 3). The increase in the narrow pores fraction between sample IV and sample III is probably behind the constancy of A_{BET} (Table 1). On the other hand, the further increase of ZnO caused a general decrease in the pore dimensions, as reflected by the value of r_H, making the existing narrow pores furnish a lower area, as appeared from the vast decrease in area between samples III and II.

SiO_2–ZnO(600)

Unlike silica(600), all isotherms in this group were of type II, with closed hysteresis loops that showed variance in their closure point (Table 2). The area and pore volume decreased successively, so that r_H varied directly with ZnO content up to 70%.

The *V vs. t* plots reflected that the addition of ZnO caused the pore system to behave differently upon heating (Fig. 2). Thus, at 15% ZnO (Sample V) some pore narrowing occurred, which made the mesopores of very limited sizes. A further increase of ZnO resulted in larger mesopores and the narrow pores probably also increased. The latter were increasingly reduced at higher ZnO contents, and at 85% ZnO measurable narrow porosity was no longer present. The increase in pore dimension can also be seen from the value of r_H (Table 2).

The coexistence of narrow pores is concluded from the cumulative data obtained from pore size analysis (Table 2), and the change in the narrow pore fraction as a function of SiO_2 content is depicted in Fig. 3. The marked increase in pore dimensions between sample V and sample IV probably resulted in the enclosing of more narrow pores, as reflected by the increase in the fraction of area contained in narrow pores. The implication is that, on increase of the ZnO content from 15 to 30%, a maximum relative pore widening took place simultaneously with a maximum measurable pore narrowing. The *V vs. t* plot for sample IV (30% ZnO) showed a delay in the upward deviation (t=7.0 Å, i.e. p/p^o=0.65), which can be understood to result from a partial compensation effect. These changes in pore dimensions explain the increases in V_p and BET C-constant for sample IV (Table 2).

Sintering can occur by movement of bulk material from the surface of wide capillaries to fill them in smaller ones, so that the average pore size is increased. A temperature of 300°C, nearly midway to the sintering temperature of silica [16], resulted in a general pore narrowing. Reductions in the number and the size of the mesopores created groups with narrower sizes, whose effect compensated the expected effect due to the disappearance of the narrow pores originally present. This appeared as a decrease in V_p, but not in A_{BET}, because the small pores have a high area to volume ratio. The addition of ZnO enhanced the process of pore narrowing upon heating, which is reflected by decreases in both V_p and A_{BET}. However, this pore narrowing did not proceed monotonously, in the sense that it adopted two ranges of pore size. The size that predominated at 30% ZnO (sample IV) became narrower at higher ZnO contents, and at 85% ZnO (sample I) no measurable (by N_2) narrow pores were present.

Heating at 600°C caused the bulk material to move so that the very small pores were closed and the losses in area and pore volume which resulted were compensated through the changes that took place in the larger pores. Pore widening made the pores deep as well as wide, making them furnish more volume and area to be measured; this equalized (or over equalized) the losses expected from the changes in the narrow pores. The presence of ZnO may prevent the bulk material from moving in this way, and consequently decreases in area and volume occurred.

At both heating temperatures, the decrease in volume upon ZnO addition was more important than that in area, and the effects were always more evident at the higher temperature. At both heating temperatures, sample IV (30% ZnO) seemed to possess a pore structure that represents a transient state through the flux of pore system change.

The IR spectra in the 'window' region of silica [17] (Fig. 4) for the (300) series as representative the (600) series give similar spectra show that sample IV exhibits broader absorption in the region 1200–1000 cm^{-1}, attributed to asymmetric stretching of Si–O–Si bonds, due to the motion of oxygen [18, 19], and an increased intensity of the band at ~800 cm^{-1}, attributed to symmetric stretching of Si–O–Si links, due to the motion of Si atoms [18]. The shoulder at ~1200 cm^{-1} and the band at 800 cm^{-1} are further classified as external linkage-structure sensitive [20]. The appearance of a shoulder at ~1200 cm^{-1} is attributed to more oblate particles [19], the broadness of the band in the region 1200–1000 cm^{-1} is correlated with variable range of Si–O bond environment [21], and finally the increase in intensity of the bands at ~1200 and 800 cm^{-1} was found to correspond to a decrease in the silica density [22]. This reflects the changes induced in the pore structure of silica upon addition of ZnO, which correlated especially with the changes recorded at 30% ZnO (sample IV).

At temperatures such as 300 or 600°C, no solid-state interactions that may result in spinel formation (Zn_2SiO_4) are expected, since the melting point of ZnO is about

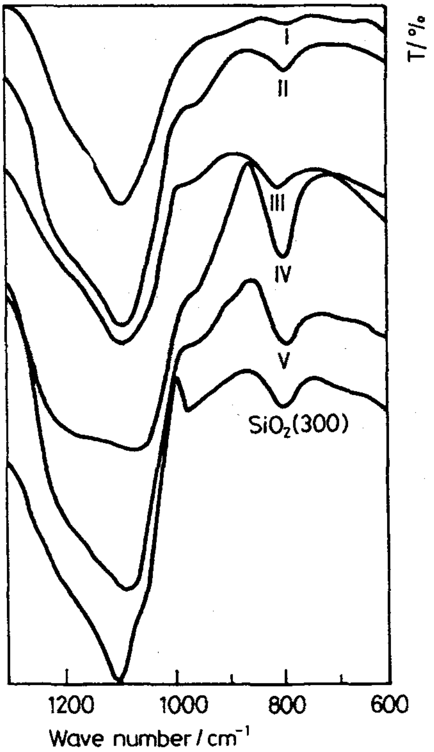

Fig. 4 IR spectra of SiO_2–ZnO (300) series

2100°C [23], and accordingly its Tamman temperature is about 900°C. The spinel was detected in our case (by X-ray) only upon heating at a temperature as high as 1000°C, and its formation was more favourable (conductivity measurements) in the range of composition 15–50% ZnO, after which ZnO seemed to be in excess, resulting in a lower extent of spinel formation. These changes in the pore structure of silica at 300 and 600°C could be correlated with reactions that take place at higher temperatures that permit solid-state reactions to occur. A spinel phase in formed at contact points, and there will always be a flux of matter across the $ZnO–Zn_2SiO_4–SiO_2$ phase boundaries. The diffusion of atomic particles encounters a resistance both in the phase boundary and in the spinel phase, so that a discontinuity in the activity of the particles occurs. For a very small spinel thickness, its diffusional resistance is negligible and the discontinuity of the activity at the phase boundary takes on the maximum value, making the reaction rate completely determined by the resistance of the phase boundary. As the thickness of the spinel layer increases, its diffusional resistance increases, and as the formation of Zn_2SiO_4 requires 2 moles of ZnO for each mole of SiO_2, the thickness of the spinel layer increases with increasing ZnO content, which decreases the extent of further spinel formation at higher ZnO contents. The fact that at 85% ZnO the pore structure of silica appeared to be independent of temperature supports the idea that at that high content of ZnO the pore system of silica is full (due to excess ZnO), so that the bulk material is inhibited from showing any reflex toward heating, and consequently the remaining pores exhibited dimensions similar to those originally present in the unheated silica.

References

1 K. Hauffe, 'Reaktionen in und an festen Stoffen'-2nd Ed., Springer-Verlag-Berlin 1966.
2 H. Schmalzried, Ber. Dtsch, Keram. Ges. 42 (1965) 11.
3 J. S. Armijo, J. Oxidation of Metals 1 (1969) 171.
4 H. Schmalzried, 'Solid State Reactions' Acad. Press Inc.-N. Y., London 1974.
5 R. Sh. Mikhail, T. El-Nabarawy and A. M. Youssef, Surf Technol., 11 (1980) 279.
6 S. Brunauer, L. S. Deming, W. S. Deming and E. Teller, J. Am. Chem. Soc., 62 (1940) 1723.
7 IUPAC Reporting Physisorption Data for Gas/Solid Systems, Pure Appl. Chem., 57 (1985) 603.
8 A. Lecloux and J. P. Pirard, J. Colloid Interface Sci., 70 (1979) 265.
9 S. Brunauer, R. Sh. Mikhail and E. E. Bodor, ibid., 24 (1967) 451.
10 a) J. H. De Boer and B. C. Lippens, J. Calal., 3 (1964) 38.
b) J. C. P. Broekhoff and J. H. De Boer, ibid., 10 (1968) 377.
11 S. J. Gregg and K. S. W. Sing, 'Adsorption, Surface Area and Porosity'-2nd Ed., Acad. Press Inc. N. Y.-London 1982, p. 233.
12 R. Sh. Mikhail, J. Chem UAR., 6 (1963) 27.
13 J. H. De Boer, The Structure and Properties of Porous Materials'-D. H. Everett and F. S. Stone (Eds)-Butterworths-London 1958.
14 R. Sh. Mikhail and F. A. Shebl, J. Colloid Interface Sci., 38 (1972) 35.
15 B. C. Lippens and J. H. De Boer, J. Catal., 4 (1965) 319.
16 J. J. Fripiat and J. Uytterhoeven, J. Phys. Chem., 66 (1962) 800.
17 B. A. Morrow and I. A. Cody, J. Phys. Chem., 80 (1976) 1995.
18 E. R. Lippincott, A. Von Volkenberg, C. E. Weir and E. N. Bunting, J. Res. Nath. Bur. Std. A61 (1958) 61.
19 A. Burneau, O. Barres, J. P. Callas and J. C. Lavalley, Langmuir, 6 (1990) 1364.
20 E. M. Flanigen, H. Khatami and H. A. Szymanski, Adv. Chem. Ser., 101 (1971) 201.
21 V. C. Farmer, A. R. Fraser and J. M. Tait, Geochimica et Cosmochimica Acta, 43 (1979) 1417.
22 J. J. Fripiat, A. J. Leonard and N. Barake, Bull. Soc. Chim. Fr., (1963) 122.
23 G. Parravano and M. Boudart, Adv. Catal. Vol. VII, (1955) 53.